

Cool Copper Template for the Formation of Oriented Nanocrystalline  $\alpha$ -Tantalum

Clare Yong,<sup>†</sup> Bei Chao Zhang,<sup>‡</sup> Chim Seng Seet,<sup>‡</sup> Alex See,<sup>‡</sup> Lap Chan,<sup>‡</sup> John Sudijono,<sup>‡</sup> San Leong Liew,<sup>‡</sup> Chih-Hang Tung,<sup>§</sup> and Hua Chun Zeng<sup>\*,†</sup>

Department of Chemical and Environmental Engineering, Faculty of Engineering, National University of Singapore, 10 Kent Ridge Crescent, Singapore 119260, Chartered Semiconductor Manufacturing, 60 Woodlands Industrial Park D, Street 2, Singapore 738406, and Institute of Microelectronic Engineering, 11 Science Park Road, Singapore Science Park II, Singapore 117685

Received: August 1, 2002; In Final Form: October 15, 2002

Ta/Cu is a strategic material combination for ultra-large-scale integrated wafer technology. Here we report an unconventional method for the synthesis of a [110]-oriented nanocrystalline  $\alpha$ -Ta thin film on freshly prepared Cu(111) templates at  $<50^\circ\text{C}$  without any redundant underlayers and post-growth treatments. The crystallite size of the  $\alpha$ -Ta-containing thin film is in the range of only 6–8 nm, and the Ta film resistivity is reduced significantly from  $186\ \mu\Omega\ \text{cm}$  down to  $104\ \mu\Omega\ \text{cm}$  with this novel method.

As ultra-large-scale integrated (ULSI) devices extend into deep submicron generations, new interconnecting schemes and materials are essential to drive performance and reliability.<sup>1,2</sup> Owing to its lower bulk electrical resistivity ( $2.2\ \mu\Omega\ \text{cm}$ ) and higher electromigration resistance, copper has begun to displace aluminum as the interconnecting material of choice.<sup>2–4</sup> Nonetheless, copper is a fast-migrating species in silicon-based devices, and its inherent chemical reactivity renders it susceptible to oxidation and corrosion.<sup>5,6</sup> Hence, the key to integrating the copper interconnecting technology is a suitable encapsulant that can act both as an effective barrier to copper diffusion and as an adhesion promoter to the surrounding dielectrics while maintaining the overall performance.<sup>2–7</sup> Tantalum and its related compounds such as tantalum nitride and tantalum silicon nitride have attracted much attention in their role as copper diffusion barriers. Being a refractory metal, tantalum is also relatively immiscible with copper and is thus an excellent barrier material for ULSI applications.<sup>2,8–14</sup> In particular, body-centered-cubic  $\alpha$ -Ta is preferred because its bulk resistivity ( $12\text{--}60\ \mu\Omega\ \text{cm}$ ) is much lower than that of metastable tetragonal  $\beta$ -Ta ( $170\text{--}210\ \mu\Omega\ \text{cm}$ ; space group  $P4_2/mnm$ ).<sup>15,16</sup> Since  $\beta$ -Ta is a common resultant phase on most substrates, attempts have been made to control the formation of  $\alpha$ -Ta, which includes using TaN, Ti, Al, and Cr underlayers, bias sputtering, high substrate temperature ( $>600^\circ\text{C}$ ), high-temperature annealing, stress relaxation, and impurity effects.<sup>2,8–14</sup> In this letter, we report a novel synthetic scheme for  $\alpha$ -Ta. Unlike the common wisdom in the  $\beta \rightarrow \alpha$  conversion, highly [110]-oriented nanocrystalline  $\alpha$ -Ta has been prepared successfully on the “cool” Cu(111) template at  $<50^\circ\text{C}$  without any redundant underlayers or post-growth treatments.

As depicted in Figure 1a, a 250-nm-thick layer of  $\text{SiO}_2$  was deposited on a Si substrate using plasma-enhanced chemical vapor deposition. Subsequently, 150-nm Cu and 25-nm Ta were deposited in succession with an ionized metal plasma technique at “standard” ( $100 < T/^\circ\text{C} < 200$ ) and “cool” ( $25 < T/^\circ\text{C} <$

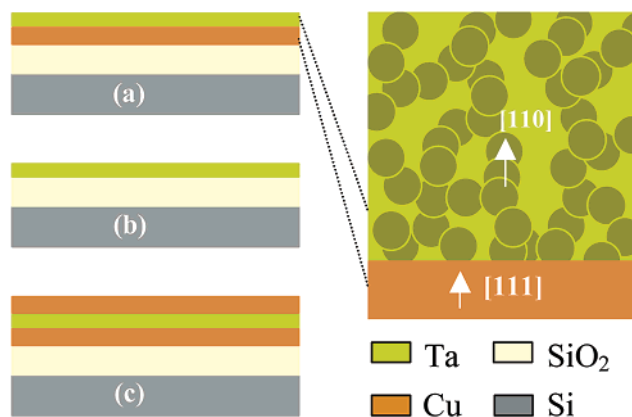


**Figure 1.** Schematic drawings of the film stacks investigated in this work. Filled circles represent  $\alpha$ -Ta nanocrystallites in the Ta/Cu interface with the  $\beta$ -Ta phase as the background.

50) conditions for Ta deposition. The film composition was confirmed with EDX. The Ta/Cu interface and microstructure were examined by high-resolution transmission electron microscopy (HRTEM, Philips FEI-CM200) and Rutherford backscattering spectroscopy (RBS), and the phase analysis was performed with X-ray diffraction (XRD, Shimadzu 6000) and electron diffraction (ED).<sup>17</sup> Similarly, 250-nm  $\text{SiO}_2$  thin films on Si were overlaid with 25 nm of Ta (Figure 1b), TaN, and Ta/TaN, respectively, to serve as references.

Figure 2 reports representative XRD patterns for the prepared film stacks. Strong Cu(111) texture is observed, as indicated by the intensity of (111) diffraction (compared to (200) diffraction). More surprisingly, whereas the standard method produces only  $\beta$ -Ta, a significant increase in the  $\alpha$ -Ta population can be achieved by using a cooler Cu substrate whose content is almost equal to that prepared with an extra TaN underlayer (i.e., Ta/TaN/ $\text{SiO}_2$ /Si).<sup>9</sup> Furthermore, the resultant  $\alpha$ -Ta is highly oriented along the [110] direction, which is evidenced in its ( $hh0$ ) reflections ( $2\theta = 38.51$  and  $82.55^\circ$ ). The lattice template of the cool Cu(111) on the  $\alpha$ -Ta formation is compared in our XRD investigations (not shown) on Ta/ $\text{SiO}_2$ /Si film stacks (Figure 1b) prepared under exactly the same conditions as those used with the Cu underlayers (Figure 2). No  $\alpha$ -Ta can be

\* To whom correspondence should be addressed. E-mail: chezhc@nus.edu.sg.

<sup>†</sup> National University of Singapore.

<sup>‡</sup> Chartered Semiconductor Manufacturing.

<sup>§</sup> Institute of Microelectronic Engineering.

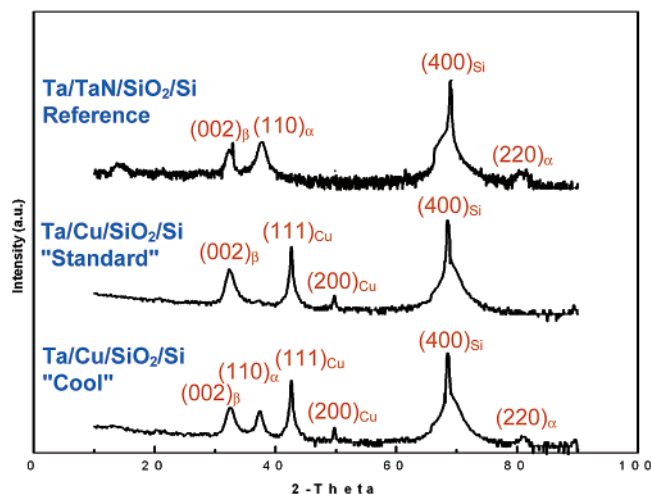


**Figure 2.** XRD patterns (log intensity) for the various film stacks in Figure 1.

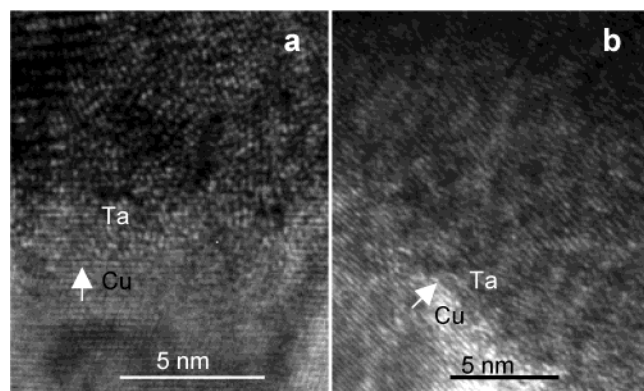


**Figure 3.** Cross-sectional TEM images of (a) the  $\beta$ -Ta/Cu interface (standard) and (b) the  $(\alpha + \beta)$ -Ta/Cu interface (cool). Arrows indicate the [111] direction of the Cu substrate.

detected with a  $\text{SiO}_2$  underlayer, indicating that the formation of  $\alpha$ -Ta is also template-specific.

The above template effect of Cu is further elucidated in our HRTEM investigation. The cross-sectional TEM images in Figure 3 reveal clean Ta/Cu interfaces with no visible interfacial diffusion or reaction (also verified by RBS tests; not shown). The film thickness of the as-deposited Ta is 27.2 and 27.7 nm, respectively, with the standard and cool processes. The Cu(111) texture can be observed clearly from the lattice fringes of  $d_{111}$  ( $2.2 \text{ \AA}$ ).<sup>2</sup> One important difference is that  $\beta$ -Ta crystallite grains in the overlayer grown with the standard process are larger and randomly arranged ( $c = d_{001} = 5.3 \text{ \AA}$ ,  $c/2 = d_{002} = 2.6 \text{ \AA}$ ,  $d_{330} = 2.4 \text{ \AA}$ ;<sup>15,16</sup> Figure 3a), whereas those prepared by the cool technique are much smaller and aligned parallel with the underlying Cu; we note that lattice fringes of both  $\beta$ -Ta ( $d_{002} = 2.6 \text{ \AA}$ ) and  $\alpha$ -Ta ( $d_{110} = 2.3 \text{ \AA}$ ) can be observed at the same time (Figure 3b).<sup>2,15,16</sup> The plan views of the crystallite grains prepared by the two different methods are displayed in Figure 4. In contrast to the Ta films prepared by the standard method, the cool Cu template yields crystallites of uniform size, in the range of 6–8 nm for both  $\beta$ - and  $\alpha$ -Ta. On the basis of the relative peak intensities/areas in the XRD patterns, the crystallite populations of  $\beta$ -Ta and  $\alpha$ -Ta are comparable. As a reaffirmation, the aligned Ta crystallites give weaker ED rings except for the  $(hh0)_\beta$  and  $(hh0)_\alpha$  diffractions (the central rings, Figure 4b) because the incident electron beam is essentially perpendicular to the  $\beta$ -Ta(002) and  $\alpha$ -Ta(110) planes.

In excellent agreement with the above results, our electrical

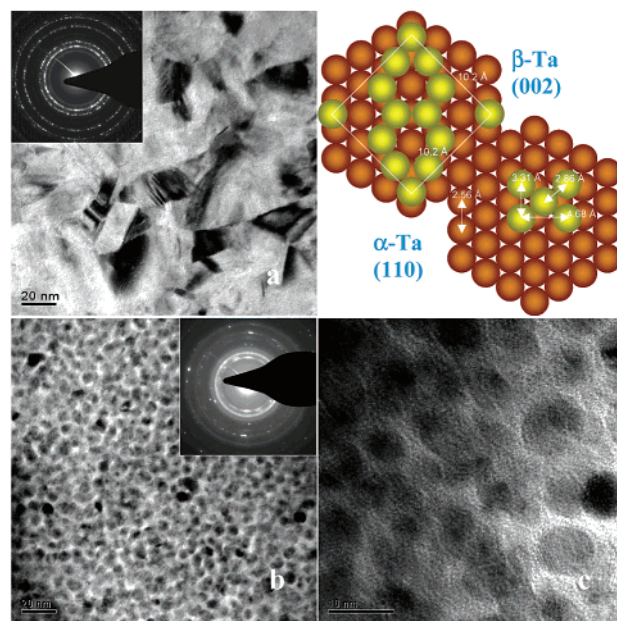


**Figure 4.** Plan-view TEM images and ED patterns for (a) the  $\beta$ -Ta thin film (standard) and (b, c) the nanocrystalline ( $\alpha + \beta$ )-Ta thin film (cool). Lattice mismatches of  $\beta$ -Ta(002) (11 Ta atoms of the tetragonal unit cell at an elevation of  $z/c = 0$ ) and  $\alpha$ -Ta(110) (2 Ta atoms of the surface unit cell) with respect to the Cu(111) template (orange atoms) are also illustrated.

resistivity measurements indicate a significant reduction (44%) in the Ta film resistivity from  $186 \mu\Omega \text{ cm}$  (standard; Ta thickness: 16.5 nm) to  $104 \mu\Omega \text{ cm}$  (cool; Ta thickness: 23.0 nm) with dual damascene architecture (or equivalent to Figure 1c). We attribute this reduction in resistivity to the presence of the oriented nanocrystalline  $\alpha$ -Ta in the latter case.

Regarding the formation of highly oriented  $\alpha$ -Ta, the template effect of the Cu(111) texture must have played an important role. It is well known that Cu can be preferentially grown along the [111] direction on a  $\beta$ -Ta(002) underlayer with a misfit strain of about 7.6%.<sup>2</sup> As indicated in Figure 4, heating will reduce this lattice mismatch and promote the growth of  $\beta$ -Ta(002), as normally observed for the standard process (Figures 3a and 4a). With our low-temperature approach, the growth of large  $\beta$ -Ta crystallites has been suppressed because of the misfit strain ( $\sim 7.6\%$ ). Although the lattice mismatch between  $\alpha$ -Ta(110) and Cu(111) is as large as 11.7% (the nearest distance between two metal (either Ta or Cu) atoms; Figure 4), the pseudo-hexagonal epitaxial growth of  $\alpha$ -Ta(110) on the (111)-textured Cu would become competitive when the  $\beta$ -Ta growth is retarded; we note that the planar atomic density of  $\alpha$ -Ta(110) is higher ( $7.75 \text{ \AA}^2/\text{Ta}$ ) than that of  $\beta$ -Ta(002) ( $9.46 \text{ \AA}^2/\text{Ta}$ ). Another plausible mechanism is the size effect; the transformation of  $\beta$ -Ta into  $\alpha$ -Ta may be facilitated by their nanodimensions, which will be further investigated.

In summary, we have devised an unconventional method for the synthesis of a [110]-oriented nanocrystalline  $\alpha$ -Ta thin film on a fresh Cu(111) template without any redundant underlayers and post-growth treatments. The simple material combination (Ta/Cu) and the low-temperature synthetic schemes will benefit future ULSI manufacturing significantly.

**Acknowledgment.** We thank the Ministry of Education for research grant R-279-000-064-112 and Kun Li, Dennis Tan, and Alfred Chong for fruitful discussions.

## References and Notes

- (1) (a) Jung, T.; Schlittler, R.; Gimzewski, J. K.; Himpfel, F. J. *Appl. Phys. A* **1995**, *61*, 467. (b) Nichols, R. J.; Kolb, D. M.; Behm, R. J. *J. Electroanal. Chem.* **1991**, *313*, 109. (c) Zach, M. P.; Ng, K. H.; Penner, R. M. *Science (Washington, D.C.)* **2000**, *290*, 2120.
- (2) (a) Kwon, K. W.; Ryu, C.; Sinclair, R.; Wong, S. S. *Appl. Phys. Lett.* **1997**, *71*, 3069. (b) Kwon, K. W.; Lee, H. J.; Sinclair, R. *Appl. Phys. Lett.* **1999**, *75*, 935.
- (3) Hwang, S.; Oh, I.; Kwak, J. *J. Am. Chem. Soc.* **2001**, *123*, 7176.
- (4) Jiang, P.; Cizeron, J.; Bertone, J. F.; Colvin, V. L. *J. Am. Chem. Soc.* **1999**, *121*, 7957.
- (5) Zeng, H. C.; McFarlane, R. A.; Mitchell, K. A. R. *Phys. Rev. B* **1989**, *39*, 8000.
- (6) Zeng, H. C.; Mitchell, K. A. R. *Surf. Sci.* **1990**, *239*, L571.
- (7) Chan, H. Y. H.; Takoudis, C. G.; Weaver, M. J. *J. Am. Chem. Soc.* **1999**, *121*, 9219.
- (8) Catania, P.; Roy, R. A.; Cuomo, J. J. *J. Appl. Phys.* **1993**, *74*, 1008.
- (9) (a) Chen, G. S.; Lee, P. Y.; Chen, S. T. *Thin Solid Films* **1999**, *353*, 264. (b) Chen, G. S.; Chen, S. T.; Huang, S. C.; Lee, H. Y. *Appl. Surf. Sci.* **2001**, *169/170*, 353.
- (10) Clevenger, L. A.; Mutscheller, A.; Harper, J. M. E.; Cabral, C., Jr.; Barmak, K. J. *Appl. Phys.* **1992**, *72*, 4918.
- (11) Schwartz, N.; Feit, E. D. *J. Electrochem. Soc.* **1977**, *124*, 123.
- (12) Hoogeveen, R.; Moske, M.; Geisler, H.; Samwer, K. *Thin Solid Films* **1996**, *275*, 203.
- (13) (a) Yoon, D. S.; Baik, H. K.; Kang, B. S.; Lee, S. M. *J. Appl. Phys.* **1996**, *80*, 6550. (b) Kwak, J. S.; Baik, H. K.; Kim, J. H.; Lee, S. M. *Appl. Phys. Lett.* **1998**, *72*, 2832.
- (14) Lee, K. W.; Lee, S.; Park, J. W. *J. Electrochem. Soc.* **2001**, *148*, C131.
- (15) Moseley, P. T.; Seabrook, C. J. *Acta Crystallogr., Sect. B* **1973**, *29*, 1170.
- (16) Dickins, G. J.; Douglas, A. M. B.; Taylor, W. H. *Acta Crystallogr.* **1956**, *9*, 297.
- (17) Sampanthar, J. T.; Zeng, H. C. *J. Am. Chem. Soc.* **2002**, *124*, 6668.